Macromol. Symp. **2011**, 302, 245–256 DOI: 10.1002/masy.201000067

Polymerisation of Butyl acrylate in the two Phase Slug Flow Regime of Parallel Microcapillary Reactors

M. Mendorf,[*1] A. Moenter,[1] T. Moll,[2] D.W. Agar,[1] J. Tiller*[2]

Summary: The potential and problems of conducting a free radical polymerisation in parallel capillary reactors are presented. By operating in the so-called slug flow regime of immiscible liquid-liquid flow, one can achieve perfectly uniform residence times which are inaccessible using single phase flow. The excellent performance available in microreactors can be exploited for higher throughputs through the simple expedient of numbering-up, i.e. operation of multiple similar reactors in parallel under identical hydrodynamic conditions. In practice this approach often comes to grief on the coupling between hydrodynamics and chemical reaction, for example due to the strong influence of polymerisation on viscosity. Rigorous modeling reveals that the operating conditions sought are actually unstable. Furthermore, the uniformity of flow distribution between parallel capillaries was found to be very sensitive to the manufacturing tolerances of the capillaries used in the presence of polymerisation. Two strategies for resolving such problems are discussed. In the first case, coupling between reaction and the flow distribution is suppressed by a sufficiently high pressure drop upstream of the temperature regulated reactor segments. The pressure drop necessary to achieve this decoupling was estimated by the model. An alternative technique involves an appropriately inexpensive flow control system for each individual capillary. Since commercially available microvalves and flow measurement equipment are too costly for parallelisation purposes, it is necessary to develop new components to fulfill these functions. An optical monitoring technique is presented that meets both the technical and economic criteria, and which can be readily combined with recently developed new micro valves [1].

Keywords: capillary reactor; free radical polymerisation; numbering-up

Introduction

Over the past two decades the principal benefits of microscale operation, such as rapid and thorough mixing, negligible temperature gradients, uniform processing histories and intensified interphase mass transport, have been extensively documented in a large number of publications (e.g. [2,3]). These benefits have great potential for polymerisation process applications.[4–6] In spite of this promise, instances of the industrial application of this technology remain few and far between. Closer inspection of the literature in this field reveals that the task of numbering-up is far more challenging than the pioneers of microtechnology originally anticipated. An example of a homogeneous solvent polymerisation using parallel microscale equipment is given by Iwasaki (2006).[7] On the strength of past experience with two phase slug flow in microcapillaries,[8,9] it is known that the presence of a second phase dramatically increases the complexity of the flow distribution task, since not only the

---

[1] Technical Chemistry B, Technical University Dortmund, Germany
E-mail: matthias.mendorf@bci.uni-dortmund.de
[2] Biomaterials and Polymer Science, Technical University Dortmund, Germany

flow rate but also the biphasic flow structure must be uniform.[9,10] In non-parallelised equipment, the flow is commonly controlled directly and precisely, by coriolis mass flow controllers for instance, or metered directly during delivery, as with syringe pumps). For parallelised equipment the pressure within the flow distribution unit must be monitored and held at a constant value in order to ensure the independent behaviour of individual capillaries. For example, if one channel becomes clogged, maintaining a constant overall flow rate will result in an increased flow rate in the remaining capillaries.[11]

In some cases, and in particular for polymerisation reactions, the conversion as a function of the residence time, and thus the flow rate in each capillary, strongly affects the pressure drop. In the presence of such interactions, dynamic fluctuations or even complete maldistribution can occur. The motivation for this work was to investigate polymerisation in a two phase flow and to assess the possibility of parallelisation, utilising multiple individual capillaries to achieve higher overall flow rates. Initial experiments on polymerisation in parallelised systems exhibited unsteady-state behaviour and a rigorous model was thus developed to characterise the behaviour of the parallel system qualitatively. The goal was not to predict exact molecular weights or distributions, but rather to model just the weight averaged molecular weight in order to calculate viscosities and the resulting pressure drop characteristics.

Model

The kinetic model used was based on a classical idealised polymerisation rate law. The reactions and corresponding rate equations for each step are listed in Table 1.

Table 1.
Basic reactions and rate equations for a free radical polymerisation.

Initiation	$I \xrightarrow{kd} 2I^{\bullet}$	$R_d = 2fk_d[I]$
	$I^{\bullet} + M \xrightarrow{ki} P_1^{\bullet}$	
Propagation	$P_i^{\bullet} + M \xrightarrow{kp} P_{i+1}^{\bullet}$	$R_p = k_p[P^{\bullet}][M]$
Termination	$P_i^{\bullet} + P_j^{\bullet} \xrightarrow{k_t} P_{(i+j)}$	$R_t = k_t[P^{\bullet}]^2$
	$P_i^{\bullet} + P_j^{\bullet} \xrightarrow{k_t} P_i + P_j$	

The model assumes a constant radical concentration (Bodenstein pseudo-steady-state approximation). Thus the number of radicals being generated is identical to that being consumed through termination ($R_d = R_t$). The resulting overall propagation reaction can thus be expressed as:

$$R_p = \sqrt{\frac{2fk_d[I]}{k_p^2/k_t}}[M] \tag{1.1}$$

In this ideal case, the propagation rate is first order in monomer concentration and half order with respect to the initiator concentration. By replacing the kinetic constants k_t and k_p by the single kinetic constant term k^2_p/k_t, only one temperature dependency for the polymerisation reaction and one temperature dependency for the initialisation reaction is needed. Initiator decomposition kinetics[12] and activation energies of propagation[13] and termination[14] rates are taken from the literature, while the ratio of the pre-exponential factors for propagation and termination k_t/k_p^2 were obtained by fitting experimental data.

The instantaneous molecular weight was calculated from the ratio of propagation to termination rates, taking into account the degree of coupling ξ, which indicates the amount of macromolecular termination by combination or disproportion (ξ = 1 only disproportion; ξ = 2 only combination).

$$M_{n,inst} = \xi \frac{R_p}{R_t} = \xi \sqrt{\frac{1}{2fk_d[I]k_p^2/k_t}}[M] \tag{1.2}$$

For the one-dimensional discretisation of the capillary reactor in the axial direction, fractions of the newly formed polymer n_i and m_i and the instantaneous molecular weight $M_{n,inst}$ were calculated. By the numerical integration over all previous discretised volumes it was possible to ascertain the number and weight averaged

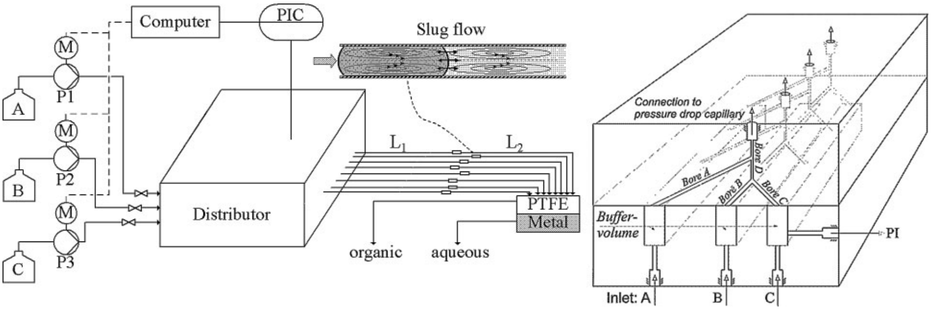

Figure 1.

molecular weight in their original form:

$$\overline{M}_W = \alpha \frac{\sum_i^\infty m_i M_i}{\sum_i^\infty m_i} \tag{1.3}$$

$$\overline{M}_n = \frac{\sum_i^\infty n_i M_i}{\sum_i^\infty n_i} \tag{1.4}$$

Additionally, the factor $\alpha=2$ was employed, because even under isothermal and constant concentration conditions for all free radical polymerisation reactions the narrowest molecular weight distribution which can be achieved is the Schulz-Flory distribution with a PDI (polydispersity index = Mw/Mn) of 2 or more.

Of course the kinetic model is not able to predict the correct results for polymerisation over a wider range of different reaction conditions, than that used for the kinetic fit, but it is nevertheless good enough to predict the qualitative influences of temperature and residence time. However, it neglects any effect of increasing viscosity on kinetic constants or the underlying polymerisation mechanism, such as backbiting, termination by transfer, branching etc. with have been reported in the literature on acrylate polymerisations (e.g.[14–16]).

Figure 2 shows clearly, that the fitted kinetic model matches the experimental

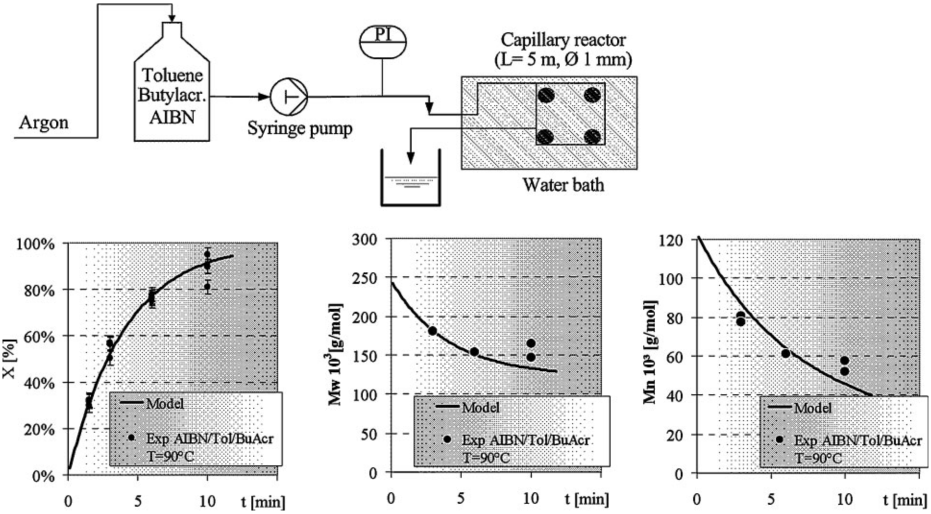

Figure 2.

Table 2.
Viscosity model equations.

η of pure liquids	$\ln(\eta_i[Pas]) = a_1 + a_2/T[K] + a_3T[K] + a_4T[K]^2 + a_5T[K]^3$	(1.5)	[17]
η of pure polymer	$\eta_{polymer}[Pas] = b_1\left(M_w[g/mol]/b_2\right)^{\alpha}\exp\left(\frac{Ea_\eta}{R}\left(\frac{1}{T[K]} - \frac{1}{b_3}\right)\right)$	(1.6)	[18]
η of mon./solvent	$\eta_{solv/mon}[Pas] = (m_{solv}\cdot\eta_{solv} + m_{mon}\eta_{mon})^1/(m_{solv} + m_{mon})$	(1.7)	
η of polymer solution	$+\left[c_1 + c_2(1-c_3w_p)\right](1-w_p)w_p\ln\ln\eta_{solv/mon}$	(1.8)	[18]
Non-Newtonian η	$\eta_{mix} = \eta_{0,mix}\left[1 + \left(\frac{\eta_{0,mix}\cdot\gamma}{d_1}\right)^2\right]^{(d_2-1)/2}$	(1.9)	[19]
Mean shear rate	$\gamma = 2\frac{u_{mean}}{R}$	(1.10)	

data well. The experiments were carried out using a single capillary (PTFE) at a temperature of T = 90 °C. AIBN ([AIBN] = 0.025 mol/l) was used as the initiator and the monomer weight fraction employed was 50%. Residence times were varied using different flow rates by means of a syringe pump[a]. The monomer used was purified by destillation and all solvents were stripped with argon prior to and during experimentation. The reaction was stopped by cooling down to ambient temperature, and conversions were determined by evaporation and weighing of samples. Molecular weights were measured with the help of GPC SEC[b].

Viscosity and Pressure Drop Correlations

The viscosity correlations used are listed in Table 2. The model parameters employed are listed in the appendix. The influence of shear rate on the flow behaviour was determined with a rotational viscometer[c] and the dependency of Newtonian viscosity on temperature and polymer concentrations are fitted to the experimental data measured with an Ubbelohde viscometer[d].

Because the pressure drop in parallel capillaries systems is equal for each unit, the flow rate will be a function of capillary geometry, slug structure (i.e. slug length) and the viscosity of both phases. The pressure drop of slug flow in capillaries has been studied only at low Reynolds numbers[20] or for low viscous liquids.[8,21] Under these circumstances, the liquid volumes in the vicinity of the phase interface play a dominant role, because the flow at the centre of the capillary has to be redirected due to the presence of the phase interface. Apart from this, the flow field in the bulk of the slug, especially in the continuous, i.e. wall-wetting, phase, or in long dispersed phase slugs, is similar to the parabolic laminar profiles found in homogeneous single phase flow. By visualisation of the circulation, the only difference is the displacement of the coordinate system, which moves with the mean slug velocity (see Figure 3, modified from).[22] With increasing viscosity the impact of viscous friction in the bulk liquid on pressure drop increases. As a result, the very simple Hagen-Poiseuille calculation (see equation 1.11, with a mass averaged viscosity of both phases) provides adequate pressure drop

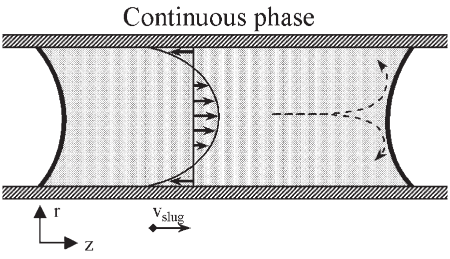

Figure 3.

---

[a] Labortechnik Heinz Seewald, LDP 5 precision pump

[b] MZ GEL SDplus, linear 5μm; solvent chloroform; T=30°C; detector RI 3580

[c] Haake Rotovisco RV20

[d] KPG Ubbelohden Viskosimeter

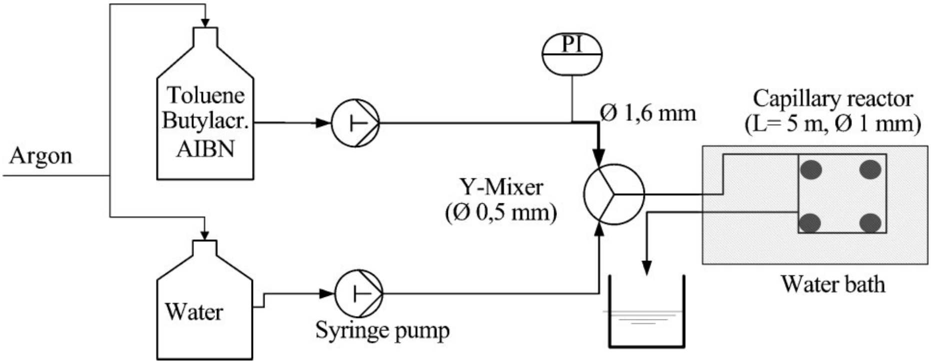

Figure 4.

values for viscosities greater than 10 mPa s.

$$\Delta p = \frac{8Q\eta_{mean}L}{\pi R^4} = \underbrace{\frac{8L}{\pi R^4}}_{K_{Laminar}}\eta Q \qquad (1.11)$$

Using the Hagen-Poiseuille law for the pressure drop calculation, the flow rate Q can be expressed as a function of the pressure drop, the viscosity and a geometric factor $K_{Lamninar}$. The fourth order dependence on the radius shows clearly that manufacturing tolerances will strongly affect deviations from uniform flow distribution in parallel capillary systems.

Comparison of Experimental and Simulation Results

The experimental set-up is depicted in Figure 4. The pressure was measured upstream of a Y-mixer into which the liquids were introduced by two non-pulsating syringe pumps. In contrast to the experiments with parallel capillaries, the flow into the capillary was well-defined and constant. The pressure drop measured can thus be correlated with a given flow rate.

The pressure drops measured for different flow rates exhibited unexpected behaviour. Usually an increase of pressure drop would be expected for higher flow rates. Here, however, higher flow rates apparently only have a minor effect on the pressure drop measured. It seems that the decreased residence time for higher flow rates and thus a resulting smaller overall viscosity could even decrease pressure drop at higher flow rates (see Figure 5, left).

The predicted pressure drop values show a reasonably good agreement with the experimental data from the single capillary experiment (see Figure 5). The model

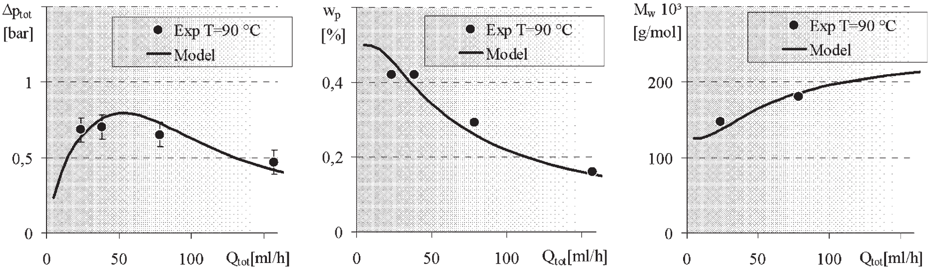

Figure 5.

confirmed the decrease of pressure drop with an increase of flow rate. No differences were observed in comparison to the homogeneous single phase flow experiments (see Figure 2) either in terms of conversion, molecular weight or its distribution. The conclusion is that under the prevailing circumstances diffusion is sufficient to suppress radial concentration gradients which might otherwise influence the polymerisation reaction in the homogeneous system. Since the timescale for generating a polymer molecule by a free radical polymerisation – a few milliseconds - is several orders of magnitude less than the residence time (minutes), the molecular weights of the polymer formed are, in contrast to living polymerisations, not directly a function of residence time in the reactor, but only depend on the axial concentration profiles of the reacting species. Due to the uniform overall velocities, these axial gradients are always the same and thus no effect was observed.

Simulation Study

The objective of the simulation was to capture the qualitative performance of parallel capillaries. Parallel capillaries are exposed to exactly the same pressure drop due to the similar pressure upstream of the flow distribution. The flow into each individual capillary cannot, however, be dictated by means of the displacement pumps as in the single capillary experiments. Since the pressure in the driving force for the capillary flow, it is used as the abscissa when illustrating the simulation results. As it can be seen in Figure 5, it is not unambiguously clear which flow rate will result for a given pressure drop. The flow rate vs. pressure drop plot with a logarithmic ordinate axis (see Figure 6 left) shows clearly that three different states are possible (e.g. markers for a pressure drop of 0.7 bar).

In Figure 6 the simulation results for three capillary reactors with a length of 5m and a diameter of 0.95 mm (id −5%, capillary a), 1 mm (id 0%, capillary b) and 1.05 mm (id +5%, capillary c) are presented. Typical variations in capillary diameter lay in the range of 1–2%, but we observed that the effect of different tightness of fitting seals on flow rates is of the same order of magnitude, therefore 5% deviation in diameter is a realistic worst case scenario for parallelised capillary systems. In Figure 6 the reactor performance desired would be a compromise between achieving a high production rate on one hand and a large polymer weight fraction or monomer conversion on the other. The problem is that for a pressure drop exceeding 0.8 bar the capillary c might have only one possible operating state with a very high flow rate and virtually no conversion due to an extremely low residence time. In this case, the monomer concentration in the whole reactor would be roughly the inlet value and thus the overall reaction rate and the production

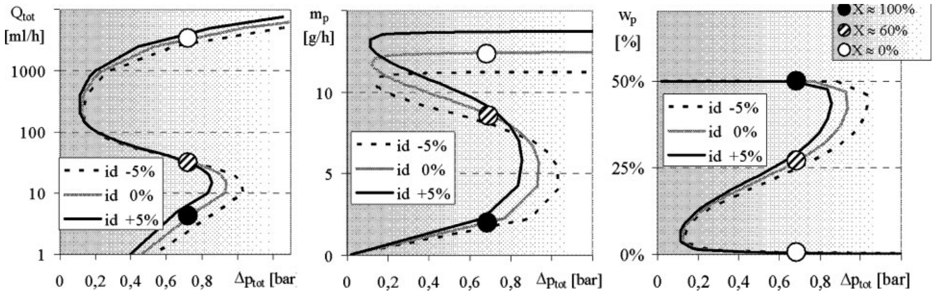

Figure 6.

rate are maximal. Of course this situation is undesirable, because of the strong diluted polymer solution that would be obtained. The other extreme is operation at nearly 100% conversion, but with very low flow rates and thus low production rates. In this state, the different capillary tolerances strongly influence overall reactor performance, giving rise to flow deviations will result in a range of 4–8 ml/h. In addition, for higher monomer concentrations, it might be expected, that such operating conditions could cause plugging. It could therefore well be, that the operating state with higher production rates but moderate conversion represents the most desirable condition. However, this operating state is unstable: small flow variations (e.g. during start-up) can lead to runaway behaviour. For example, if the flow rate falls briefly below the intermediate steady-state value, the increased residence time will result in a increased viscosity and thus the flow will progressively decrease even more with time. This will continue until the stable steady-state condition with nearly 100% conversion, but very low production rates, is reached.

By installing a capillary at ambient temperature in front of the heated main capillary reactor segment it is possible to diminish the feedback between the reaction and the hydrodynamics. With increasing length, and thus additional pressure drop, in this non-reactive section, the system becomes less unstable. Using a capillary with an inner diameter of 0.5 mm and a length of at least 20 m the desired steady-state with a flow of 38 ml/h (compared to Figure 6) is stable (see Fig. 7). The additional pressure needed is more than 100% higher than that for a single capillary without an upstream non-reactive capillary section.

Polymerisation Experiments with Parallel Capillaries

The experiments were carried out under slight different reaction conditions to those used for the single capillary experiments. The temperature was reduced to 80 °C and the monomer was diluted to 40 wt% to avoid plugging.

The set-up is illustrated in Figure 8. The organic media (toluene, butyl acrylate, AIBN) are pre-mixed and introduced via inlet B, while the inlet C was plugged. In this manner, the influence of diluted or higher monomer / initiator concentration in the organic phase is avoided, but later experimentation allowed for a separate feed for the monomer and initiator solu-

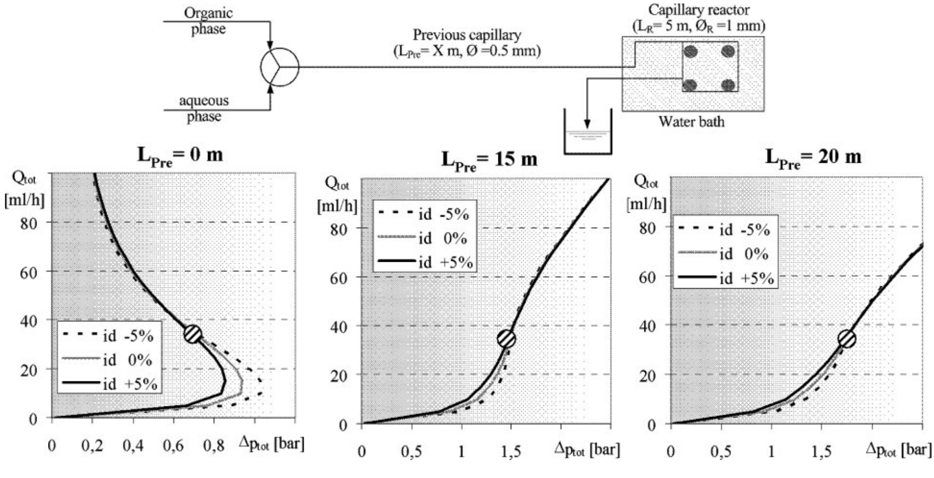

Figure 7.

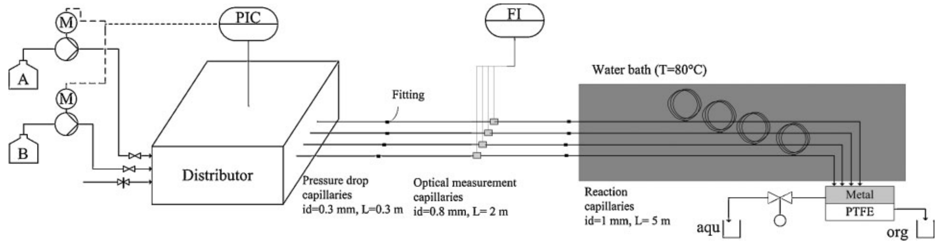

Figure 8.

tions. Downstream of the distributor, a pressure drop capillary with an internal diameter of 0.3 mm and a length of 0.3 m was installed and a further capillary with an internal diameter of 0.8 mm and a length of 2 m was used for the connection to the heated capillary reactor segment.

A new optical measurement system was installed to monitor the slug velocities in each individual capillary. A dye in the aqueous phase was used to enhance the contrast between the two phases. The optical measurement determines the step signals associated with the slug flow and by calculating the time derivative of the signals, i.e. the increase/decrease of the signal measured during the change from one phase to the other, the amplitude of which is proportional to the slug velocity (see Figure 9). To decrease the signal to noise ratio a low pass filter was used in signal processing.

Figure 10 demonstrates clearly that the unstable behaviour predicted actually

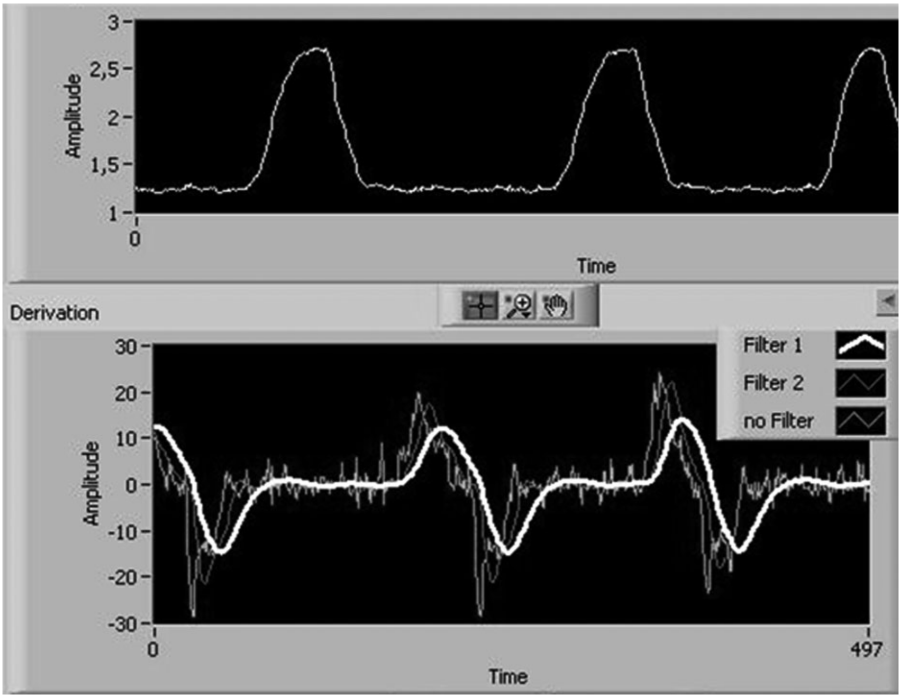

Figure 9.

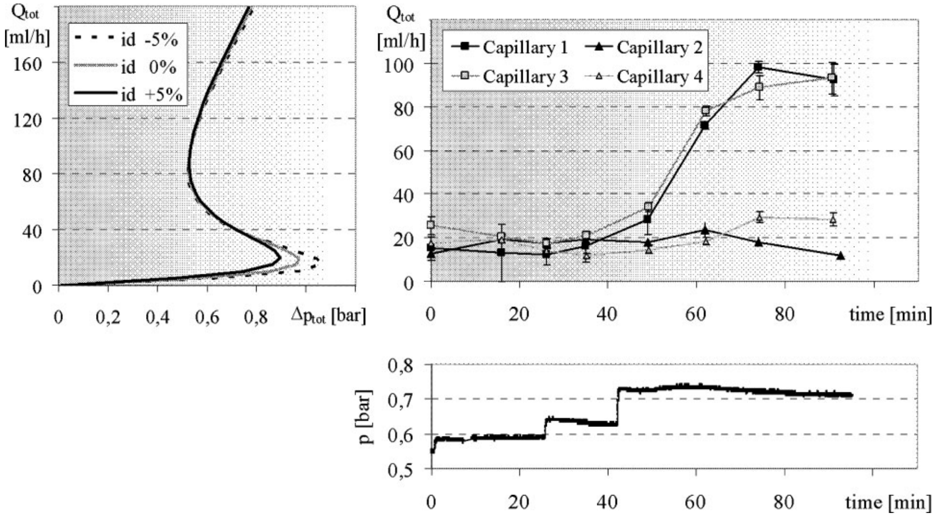

Figure 10.

occurs. During the experiment the pressure was increased with time, the goal being to achieve a flow rate of 40 ml/h. As can be seen on the left hand side of Figure 10, the pressure drop capillary did not hinder the multiplicity phenomena. The calculated pressure drop of the pressure drop capillary was about 60 mbar for 20 ml/h and around 250 mbar for 80 ml/h. After 40 minutes and an increased pressure drop of above 0.7 bar the real system shows a drift in the flow rates for capillary 1 and 3 to the stable condition at very high flow rates. The model predicted this for 5% differences in the reaction capillary diameters at pressure drops of above 0.8 bar. The predicted flow rate for low conversion and high flow rates might have been be overestimated, but the location of the transition point was estimated surprisingly well.

Summary and Conclusion

In this work a reactor model is presented to predict the behaviour of parallel capillary reactors for a butyl acrylate polymerisation. A simple kinetic model based on a classical idealized polymerisation rate law was used. The viscosity was calculated based on the polymer fraction, averaged molecular weight and mean shear force. The Hagen-Poiseuille law was used for homogeneous and two phase slug flow pressure drop calculations. Due to the high impact of viscous friction on the pressure drop in the bulk of the continuous slug phase, the simple Hagen-Poiseuille calculation is sufficient for pressure drop calculations with viscosities greater than 10 mPa s. The predicted pressure drop values showed good agreement with experimental data in the single capillary experiments. The model confirmed the existence of multiple steady-states for a given pressure drop. Since all parallel capillary reactors are exposed to the same pressure upstream of the distributor, it is not possible to predict which flow rate will result in which capillary. A simulation using +/-5% deviation in the capillary diameter was taken as a realistic estimate for a worst case scenario in a parallel capillary system. It could be shown that three steady-state flows could be attained for the same pressure drop, one of which was unstable and would thus tend revert to one of the two stable conditions upon minor disturbances. It is entirely conceivable that different steady-states can coexist in different capillaries. The multiple capillary experiments also showed that two stable conditions are possible, while the third is unstable. In particular, the predicted pressure level, at which the transition between the steady-states might occur due to manufacturing tolerances, was estimated by the model surprisingly well.

Furthermore, the model was used to calculate that an additional pressure drop in an upstream capillary of around 100% is needed to eliminate the feedback between reaction and hydrodynamics.

From these results it can be concluded, that the parallel operation of microchannel reactors elements for polymerisation processes requires a precise additional pressure drop control for each individual capillary. Since Iwasaki[7] did not report any problems with multiplicity for parallel capillaries with a very similar butyl acrylate polymerisation in homogeneous single phase flow, it can be conjectured that the distribution capillaries used, which were operated at ca. 0 °C, might have created enough pressure drop to assure a particular steady-state condition. Furthermore, this might also explain the unsuccessful operation of a second unit with parallel channels, without additional pressure drop sections before the heated reactor segments.

Outlook

The installation of precise pressure drop control units in each capillary would thus seem to be a prerequisite for reliable the process control in parallel capillary reactors for polymerisations. Since the installation of conventional commercially available microvalves entails costs of the order of a thousand Euros or more per capillary, a more appropriate and affordable new microvalve prototype has been developed (for further information see[9]). As the objective is only to fine tune the flow distribution, which is already uniform to within a deviation of less than 10%, many of the demands made on conventional microvalves become superfluous. In the near future, a new control concept will be implemented using the optical measurement technique and the new microvalve arrangement to run polymerisation reactions in parallel microcapillaries, thus enabling the exploitation of the benefits of microscale operation at higher throughputs.

Additionally a two phase polymerisation process is being investigated, in which the sensitivity to flow deviations strongly affects the molecular weight distribution (MWD). Introducing the initiator via extraction from the aqueous phase into the organic monomer phase enables manipulation of the polymerisation reaction, in which the hydrodynamics and slug flow structure play a crucial role.

Since the slugs exhibit a high specific surface area of up to 5000 m^{-1}, [18] the time needed to reach an equilibrium state with a roughly constant initiator concentration is a function of flow rate and slug structure. It is evident that the faster the initiator is extracted into the monomer phase and a

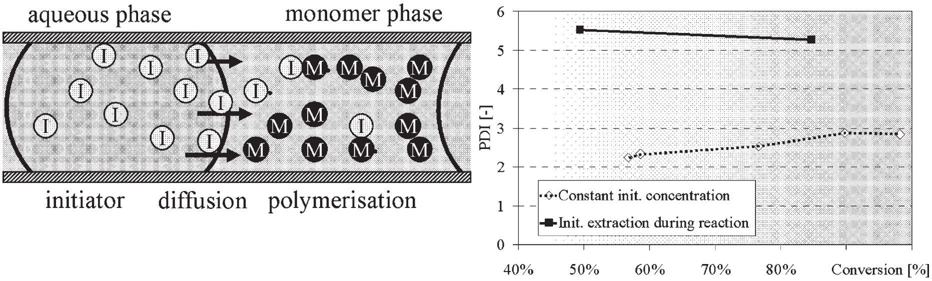

Figure 11.

constant initiator concentration is reached, the narrower the molecular weight distribution of the obtained polymer will be (see Figure 11).

Notation

R_d	initiator decomposition rate [mol/(s L)]
R_p	propagation rate [mol/(s L)]
R_t	termination rate [mol/(s L)]
[I]	concentration of species I [mol/L]
k_d	rate constant of decomposition [1/s]
k_i	rate constant of initialisation [L/(mol s)]
k_p	rate constant of propagation [L/(mol s)]
k_t	rate constant of termination [L/(mol s)]
M	molecular weight [g/mol]
η	viscosity [mPa s]
T	temperature [K]
d	diameter [m]
L	length [m]
w	weight fraction [%]
γ	shear rate [1/s]
u	velocity [m/s]
Δp	pressure drop [bar]
$K_{laminar}$	constant [$1/m^3$]
X	conversion [%]
Q	flow rate [mL/h]
I	initiator
M	monomer
$I^\bullet$	initiator radical
$P^\bullet$	polymer radical
P	terminated polymer
m	mass
w	weight
n	number
PTFE	Polytetrafluoroethylene
AIBN	Azobisisobutyronitrile
id	inner diameter
tot	total
PIC	pressure indicator controller
FI	flow indicator

parameter	value	Source
$f \cdot k_d$	$0.4 \cdot 1.58 \cdot 10^{15} [1/s] \exp(-13200/(R \cdot T))$	[12]
k_t/k_p^2	$4.2 \cdot 10^{-2} [mols/L] \exp(Ea_t - 2Ea_p)/(R \cdot T)$	this work
Ea_p	17900 [J/(mol·K]	[13]
Ea_t	5590 [J/(mol·K]	[14]
ξ	1	this work
b_1	$4.0 \cdot 10^{15}$ [Pas]	this work
b_2	450000[g/mol]	this work
α	3,17	[18]
b_3	338 K	this work
c_1	-0.38	this work
c_2	-0.22	this work
c_3	60	this work
d_1	38.87 [kg/(m s^2)]	this work
d_2	0.4836	this work

[1] M. Mendorf, H. Nachtrodt, A. Mescher, A. Ghaini, D. W. Agar, *Ind Eng Chem Res* **2010**.

[2] A. Gavriilidis, P. Angeli, E. Cao, K. K. Yeong, Y. S. S. Wan, *Trans IChemE* **2002**, *80*, p. 3–30.

[3] V. Hessel, J. C. S. A. Renken, J.-I. Yoshida, *Micro Process Engineering, Vol 3 System Process and Plant Engineering*, **2009**, Wiley-VCH Verlag GmbH & CoKGaA, Weinheim

[4] T. Bayer, *Pysall, D. Microreaction technology* **2000**, p. 165–170.

[5] T. Iwasaki, J. Yoshida, *Macromolecules* **2005**, *38*(4), p. 1159–1163.

[6] W. H. Ehrfeld, V. Löwe, H. Microreactors, *New Technology for Modern Chemistry*, **2000**, Weinheim Wiley-VCH.

[7] T. Iwasaki, N. Kawano, J. Yoshida, *Org Process Res Dev* **2006**, *10*(6), p. 1126–1131.

[8] M. N. Kashid, D. W. Agar, *Chem Eng J* **2007**, *131*(1–3), p. 1–13.

[9] M. Mendorf, H. Nachtrodt, A. Mescher, A. Ghaini, D. W. Agar, *Ind Eng Chem Res* **2010**, accepted article in press

[10] M. Mendorf, H. Nachtrodt, D. Agar, *Chem-Ing-Tech* **2010**, *82*(3), p. 259–264.

[11] O. Tonomura, T. Tominari, M. Kano, S. Hasebe, *Chem Eng J* **2008**, *135*, p. 131–S137.

[12] D. C. Timm, J. F. Scamehorn, *AIChE Symposium Series* **1976**, *72*(160), p. 43–50.

[13] J. M. Asua, S. Beuermann, M. Buback, P. Castignolles, B. Charleux, R. G. Gilbert, R. A. Hutchinson, J. R. Leiza, A. N. Nikitin, J.-P. Vairon, A. M. V. Herk, *Macromolecular Chemistry and Physics* **2004**, *205*(16), p. 2151–2160.

[14] S. Beuermann, M. Buback, *Progress in Polymer Science* **2002**, *27*(2), p. 191–254.

[15] Quan. C. **2002**.

[16] G. E. Scott, E. Senogles, *Journal of Macromolecular Science* **1974**, *8*, p. 753–773.

[17] M. Kleiber, R. Joh, *VDI Wärmeatlas*, **2006**, Springer Verlag Berlin.

[18] Y. Song, P. M. Mathias, D. Tremblay, C.-C. Chen, *Ind Eng Chem Res* **2003**, *42*(11), p. 2415–2422.

[19] M. Boildin, W. M. Kulicke, H. Kehler, *Colloid Polymer Science* **1988**, *266*, p. 793.

[20] Z. Hórvölgyi, É. Kiss, J. Pintér, *Colloids and Surfaces* **1991**, *55*, p. 257–270.

[21] M. B. Charles, *Canadian Journal of Chemical Engineering* **1963**, April, p. 46–51.

[22] G. Dummann, U. Quittmann, L. Groschel, D. W. Agar, O. Worz, K. Morgenschweis, *Catal Today* **2003**, *79*(1–4), p. 433–439.